ECCOMAS Congress 2016
VII European Congress on Computational Methods in Applied Sciences and Engineering
M. Papadrakakis, V. Papadopoulos, G. Stefanou, V. Plevris (eds.)
Crete Island, Greece, 5–10 June 2016

ASSESSMENT OF A CONTINUUM MICROMECHANICS-BASED MULTISCALE MODEL FOR CONCRETE BY MEANS OF SENSITIVITY ANALYSIS AND UNCERTAINTY PROPAGATION

Luise Göbel[1], Andrea Osburg[2], Tom Lahmer[3]

[1]Research Training Group 1462, Bauhaus-Universität Weimar
Berkaer Strasse 9, 99423 Weimar, Germany
e-mail: luise.goebel@uni-weimar.de

[2] F. A. Finger Institute for Building Material Engineering, Bauhaus-Universität Weimar
Coudraystrasse 11A, 99423 Weimar, Germany
e-mail: andrea.osburg@uni-weimar.de

[3] Institute of Structural Mechanics, Bauhaus-Universität Weimar
Marienstrasse 15, 99423 Weimar, Germany
e-mail: tom.lahmer@uni-weimar.de

Keywords: Multiscale Modeling, Concrete, Continuum Micromechanics, Uncertainty Propagation, Sensitivity Analysis, Variance Decomposition

Abstract. *In structural engineering, the behavior of materials is often defined at the macroscopic level where experiments are suitable. Utilizing the advanced knowledge of the microstructure, multiscale modeling represents a beneficial tool for material properties estimation. During the last two decades, multiscale models based on continuum micromechanics for concrete have been developed. The implementation of these multiscale models is performed in a two-step manner: First, the volume fractions of the phases at the lower scale are calculated, followed by an upscaling process. These models require a high number of input parameters which partially exhibit high uncertainties. The paper discusses the question how the uncertainties of the input parameters are propagated through the different scales of concrete during the upscaling process. It is investigated whether the upscaled mechanical properties will show a high variability due to the diversifying properties of the initial components. Sensitivity analysis is applied to cement pastes, mortars, and concretes with water-to-cement ratios of 0.40, and 0.60. The total order sensitivity indices according to the variance decomposition method by Sobol are computed for all input parameters. By means of interpretation of sensitivity indices, the importance of parameters on the model output is quantified. A more accurate a priori knowledge of the input parameters can lead to a decreased uncertainty of the upscaled results. Furthermore, the uncertainty propagation starting at two commonly applied hydration kinetics models is compared. The results show that the scatter of the model responses increases significantly during the upscaling process; hence, it should be considered in the assessment of the multiscale modeling results.*

1 INTRODUCTION

In civil engineering, the behavior of materials is mostly defined at the macroscopic level. Macroscopic models for the prediction of the materials' behavior are often empirical; therefore they contain parameters without a specific physical meaning.
Concrete is commonly handled as a homogeneous material at the macroscopic scale in prediction models. However, it behaves highly heterogeneous at the microscale. Utilizing the additional knowledge of the microstructure and the materials' chemistry, multiscale modeling represents a beneficial tool for material properties estimation. Recently, multiscale models based on continuum micromechanics have been developed and successfully applied to cementitious materials. Following the modeling philosophy in continuum micromechanics, no fitting parameters are introduced; rather, a particular physical meaning is assigned to the model parameters.
By means of multiscale models, properties regarding the elasticity, strength, and creep of concrete can be predicted using intrinsic elastic properties of the constituents and their volume fractions (e.g. [1], [2], [3]). This paper focuses on the multiscale elastic analysis. The prediction of elasticity via semi-analytical homogenization methods in the framework of continuum micromechanics is performed in a two-step manner. The calculation of the volume fractions of the phases at each scale is followed by an upscaling process. The evolution of the microstructure of cement paste during the hydration process is computed using hydration kinetics models. In this study, two commonly utilized hydration kinetics models are employed: the Powers-Acker hydration model [4], [5] and the hydration model proposed by Bernard [6] and refined by Pichler et al. [7].

Commonly, multiscale analyses are performed using a deterministic approach including established values of the input parameters. Calculations comprising the stochastic input parameters result in probabilistic multiscale analyses where the upscaled mechanical property represents a stochastic variable which is a function of the parameter variation. This seems to be useful because multiscale models require a large number of input parameters that commonly exhibit a high uncertainty. The question arises whether the upscaled mechanical properties will show an increased variability due to the diversifying properties of the initial components. The paper aims to study the propagation of uncertainties of the input parameters through the different scales of concrete during the upscaling process.
Uncertainty quantification in multiscale modeling has been rarely investigated so far. Studies have been conducted for several types of materials and with different methodologies of uncertainty quantification. Clément et al. [8] considered the uncertain nature of hyperelastic heterogeneous materials at the microscopic scale and proposed a methodology for the uncertainty quantification based on polynomial chaos representation. Vu-Bac et al. [9] proposed a stochastic multiscale method for polymer nanocomposites across four length scales and quantified the uncertainties of several input parameters using different types of sensitivity analyses. Particularly, approaches for independent as well as for correlated input parameters were introduced. Uncertainties in the multiscale modeling of concrete were investigated by Berveiller [10] and Venkovic et al. [11]. Berveiller in [10] discussed the variability of the Young's modulus of cement paste using polynomial chaos expansions. Venkovic et al. [11] computed the uncertainty propagation of a multiscale poromechanics-hydration model for concrete by means of stochastic meta-models and polynomial chaos expansions.

However, a detailed uncertainty analysis at different scales of a continuum micromechanics-based multiscale model for concrete has not been performed yet to the best of the authors'

knowledge. This study aims to assess the influence of the variabilities and uncertainties of the initial composition of cement-based materials on elastic properties across the scales. Additionally, differences in the statistical variation of the model output of two different hydration kinetics models are appraised. A framework for the application of the sensitivity analysis on probabilistic multiscale modeling for concrete is proposed. Results of the sensitivity analysis applied to cement pastes, mortars, and concretes, respectively, with water-to-cement ratios of 0.40 and 0.60 are presented.
The paper is organized as follows: First, the fundamentals of continuum micromechanics are recalled and the deterministic multiscale model is introduced. Then, probabilistic multiscale modeling is performed considering uncertainties of all input parameters. The uncertainties of the model predictions at different stages of the hydration process are computed. The parameters influencing the uncertainty most are identified, and their probability density functions at different time steps are estimated. The paper is concluded with a discussion and further recommendations.

2 DETERMINISTIC MICROMECHANICAL MODEL OF CONCRETE

Theoretical fundamentals of modeling and homogenization methods within the realm of micromechanics have been presented in the works by [12], [13], [14], [15], [16]. Subsequent investigations by [6], [17], [18][19], [1] extended the principles towards the application on cementitious materials and the upscaling of elastic, strength, and creep properties from a microscopic to a macroscopic observation level.

2.1 Micromechanical representation

Within the framework of continuum micromechanics, the concept of representative volume elements (RVE) including the separation of scales requirement is followed [20]. The microstructure of concrete cannot be resolved and described in every detail. Thus, at each scale of the multiscale model, one RVE comprising quasi-homogeneous subdomains with known physical quantities is defined [2].

The morphological model for concrete adopted here is based on [7]. The model includes four scales of observation which are shown in Figure 1. For the sake of simplicity, the shapes of all embedded phases are assumed to be sphericular. It is known that the distinction of different phases morphologies increases the accuracy of the model prediction [1].

2.2 Hydration kinetics models

There are several models describing the kinetics and the evolution of volume fractions in cement pastes during the hydration process of cement particles. The two most important and principally used models are the Powers-Acker hydration model [4], [5] (”Powers model”) and the hydration model proposed by Bernard [6], later improved by Pichler et al. [7] (”Bernard model”).

2.2.1 The Powers model

The Powers model, often denoted as the ”engineering model”, provides the volume fractions of unhydrated clinker (f_{clin}), water (f_{H_2O}), hydration products (f_{hyd}), and of air (f_{air}) at the cement paste scale as functions of the initial water-to-cement ratio (w/c) and of the degree of hydration (ξ). The latter value is defined as the mass of hydration products formed up to

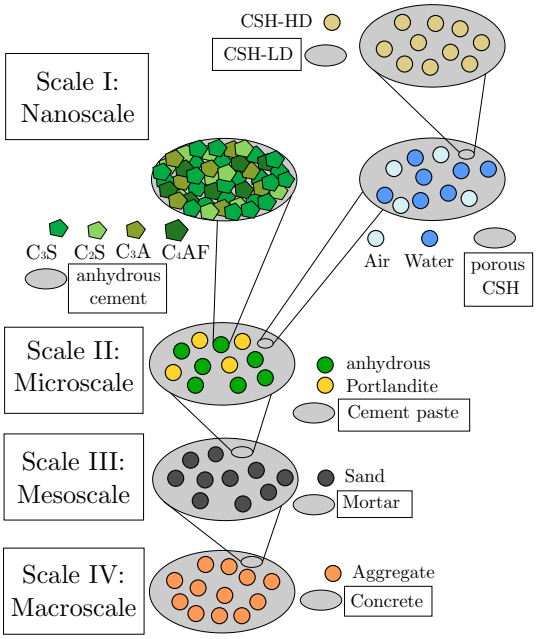

Figure 1: Scales of observation of the continuum micromechanics-based multiscale model (adopted from [7])

the current stage of the hydration process divided by the mass of hydrates formed in case of a completed hydration ($\xi = 1$). The calculation of the phase volume fractions is exemplary described in [2].

2.2.2 The Bernard model

Bernard et al. [6] proposed a hydration kinetics model which describes the evolution of relative volume properties of the elementary clinker phases. The model comprises stoichiometric and kinetic equations for the calculation of volume fractions of reactants and hydration products at different stages of the hydration. The underlying stoichiometric relations utilized in this model are adopted from Tennis and Jennings [21]. The kinetics of the hydration are described by kinetic laws that link the reaction rate $\mathrm{d}\xi/\mathrm{d}t$ to the affinity $A(\xi_x)$ as well as to kinetic constants that determine the characteristic time associated with the chemical reaction τ. Detailed information can be found in [6].

2.3 Upscaling of the elastic properties

Once the morphological model is established, the mechanical behavior of the material can be estimated using homogenization schemes. The underlying fundamentals necessary for the upscaling procedure of elastic properties can be found e.g. in [6], [17], [18][19], [1].
The self-consistent (SC) scheme [14], [15] is appropriate for polycrystalline structures, i.e., for materials which phases are dispersed in the RVE. Then, the matrix medium coincides with the homogenized medium. For materials in which a continuous matrix can be distinguished from particular inclusions, the Mori-Tanaka (MT) scheme [22], [23] is suitable. In this work, the MT scheme was applied to all RVE, except to the anhydrous cement particles. There, the SC scheme was used.
The micromechanical model estimates the elastic properties of cement pastes, mortars, and

concretes as functions of the degree of hydration and of the composition. Figure 2 shows the homogenized Young's modulus derived from multiscale modeling using the two introduced hydration kinetics models at four scales of observation. The application of the homogenization schemes yields simplified equations of the effective shear μ_{hom} and bulk modulus k_{hom} with which the Young's modulus can be computed. The respective equations can be found in [3].

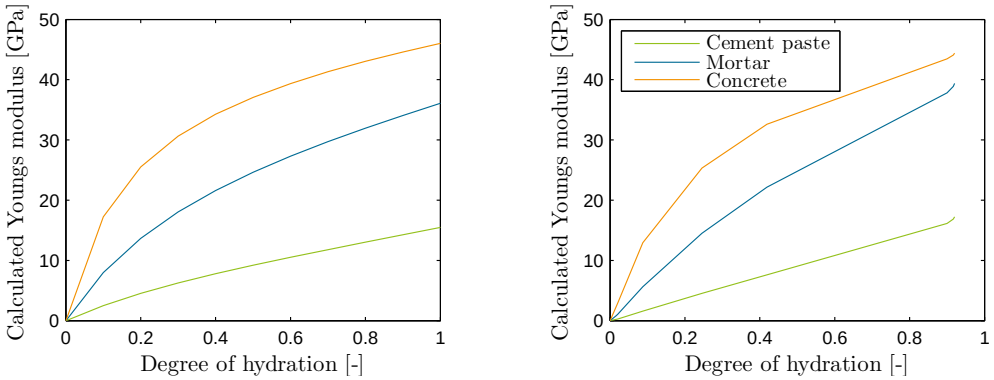

Figure 2: Deterministic Young's modulus for the Powers model (left) and the Bernard model (right) as functions of the degree of hydration calculated for a water-to-cement ratio of 0.60.

3 PROBABILISTIC MULTISCALE MODELING

Approaches for assessing the quality of the prognosis of engineering models are demanded. Methods based on uncertainty and sensitivity analyses represent suitable tools to rank input parameters according to their sensitivities on the output and to identify main contributors to the uncertainties of models. Utilizing results of these analysis helps to improve the accuracy of model predictions.

3.1 Assessment methodology

3.1.1 Sensitivity Analysis

The sensitivity analysis determines how the uncertainty of the model output can be linked to the uncertainty of the model input parameters in a qualitative and a quantitative manner. The main objectives are the identification of input parameters which have the most significant influence on the model output and the quantification of their relative importance. In subsequent modeling steps, input parameters with the least influences can be considered as deterministic, i.e. fixing a non-influential parameter at one value of its range of variance.

In this study, the variance-based global sensitivity analysis according to Saltelli [24] was applied. In contrast to local sensitivity analyses, global ones consider the simultaneous variation of all stochastic input parameters.

For a model with a scalar output Y as a function of n random input parameter sets X_i (i.e. $Y = f(X_1, X_2, ..., X_n)$), the first order sensitivity indices are calculated according to [25]:

$$S_i = \frac{V_{X_i}\left(E_{X_{\sim i}}(Y \mid X_i)\right)}{V(Y)}, \quad \sum_{i=1}^{k} S_i \leq 1, \tag{1}$$

where $V(Y)$ denotes the unconditional variance of the model output, $V_{X_i}\left(E_{X_{\sim i}}(Y \mid X_i)\right)$ is the variance of conditional expectation, and $X_{\sim i}$ identifies the matrix of all factors but X_i.

The first order sensitivity indices measure only the first order effect of X_i on the model response, i.e. the influence of every single variable in a decoupled way. Hence, higher order terms have been introduced (total effect sensitivity indices) [24]:

$$S_{T_i} = 1 - \frac{V_{X_{\sim i}}\left(E_{X_i}(Y \mid X_{\sim i})\right)}{V(Y)}, \quad \sum_{i=1}^{k} S_{T_i} \geq 1, \tag{2}$$

where $Y \mid X_{\sim i}$ is the variance of the model response caused by all input parameters X_i.
The method of Saltelli can only be applied in case of uncorrelated the input parameters. Methods considering correlated input parameters are proposed by several researchers (e.g., [26]).

3.1.2 Uncertainty Analysis

Uncertainty describes the incomplete knowledge about models and parameters. By means of uncertainty analysis, the uncertainty of the model response as a result of the uncertainty in the input parameters is quantified. There are different sources of uncertainty in the modeling process due to measurement inaccuracies, natural variations in the data, and uncertain scientific backgrounds of models.

As a first step of the uncertainty analysis, all sources of uncertainties in the input parameters that affect the model output have to be identified. The specification of model probability distributions of all input parameters is required. These distributions are either reported in the literature or are based on empirical evidence. Subsequently, the probability densitiy functions (PDF) are used to generate sample sets independently for each of the input parameters. Then, the model is evaluated with the respective parameter sets and, finally, its output is analyzed using statistical methods.

3.1.3 Sampling Approaches

Several methods are used to generate samples from given probability density functions (PDF). Some of these include the Monte Carlo Simulation (MCS), Latin Hypercube Sampling (LHS) and Advanced Latin Hypercube Sampling (ALHS).
In this study, the method of LHS has been used, since it is independent of the number of random variables. Thus, the number of required samples is significantly reduced [27]. The underlying idea of this method is the allocation of the ranges of the input parameters into intervals that have equal marginal probabilities. In the presented probabilistic multiscale model, 10,000 samples for each input parameter have been generated.

3.2 Model input parameters

The two hydration kinetics models from section 2.2 use several input parameters. In total, there are 17 stochastic input parameters for the Powers model and 26 variables for the Bernard model. All parameters are assumed to be uncorrelated.

The stochastic properties and specific values for all of the input parameters are given in detail in Appendix A.1. Due to a lack of experimental data, some probability distributions were assured by the authors which introduces bias in the results of both the uncertainty and the sensitivity analysis [11]. This represents a future topic in research.

4 RESULTS

The elastic multiscale analysis allows the prediction of the Young's modulus of cement paste, mortar, and concrete for several water-to-cement ratios at different stages of hydration. In comparison to the deterministic approach, the probabilistic analysis allows the investigation of distributions of the model responses.

4.1 Prediction of a probabilistic Young's modulus

The multiscale model was evaluated for each of the sample sets. From the stochastic model responses, the PDF and the Coefficient of Variation (CoV) of the model responses at three scales of observation were determined.
Figure 3 shows the evolution of the CoV for the two hydration kinetic models, the Powers model and the Bernard model, as functions of the degree of hydration and for different water-to-cement ratios (w/c=0.40 and 0.60).

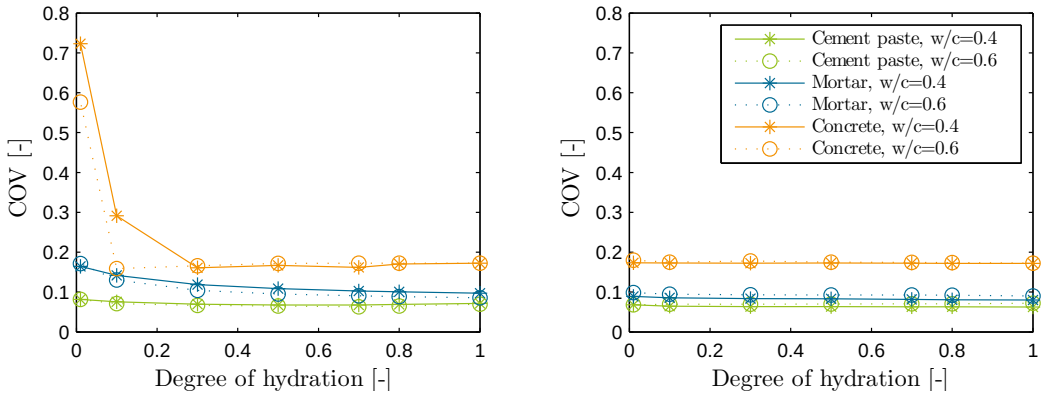

Figure 3: Evolution of the coefficient of variation of the predicted Young's modulus for the Powers model (left) and for the Bernard model (right) as functions of the degree of hydration and the w/c-ratio.

Apparently, the coefficient of variation increases during the upscaling process. At the cement paste scale, there is a fewer number of input parameters compared to the concrete scale. Thus, the CoV is the lowest at the cement paste scale. Both, the Powers model and the Bernard model, exhibit the same CoV at the fully hydrated stage. Major differences between the two hydration models occur at early hydration stages (Degree of hydration < 0.4). A higher variation in the Powers model is observed during the first stages of the hydration. In the Powers model, there are no kinetic calculations included; the volume fractions of the phases are solely functions of the w/c-ratio and the hydration degree. Since the reactions occuring in the early hydration are not described in the same detail as in the Bernard model, the model responses of Powers are constrained with larger CoV. With the advancement of the hydration process, the influence of the kinetic parameters on the Young's modulus is less significant. For the considered water-to-cement ratios, the evolutions of the CoV are almost similar to each other.

Figures 4 and 5 show the probability densities of the model responses of the two hydration kinetics model as functions of the degree of hydration. Using the 10,000 realizations of the models at different time steps, the mean, the standard deviation, and the probability distribution of the Young's modulus were estimated. The model responses of both hydration kinetic models were found to be normally distributed.

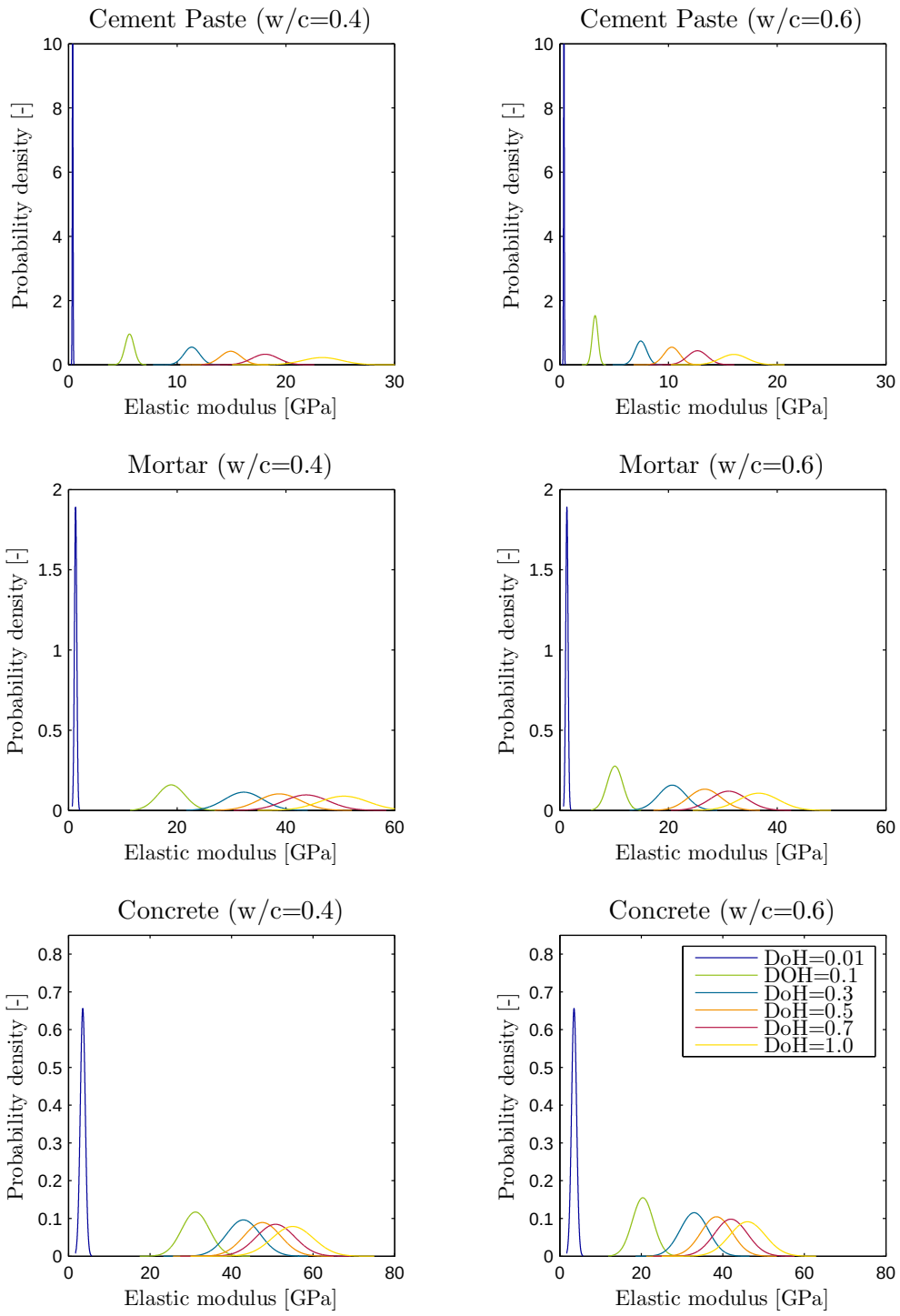

Figure 4: Probability densities of the predicted elastic modulus for the Powers model for different degrees of hydration (DoH) as well as for different w/c-ratios at the cement paste scale, the mortar scale, and the concrete scale.

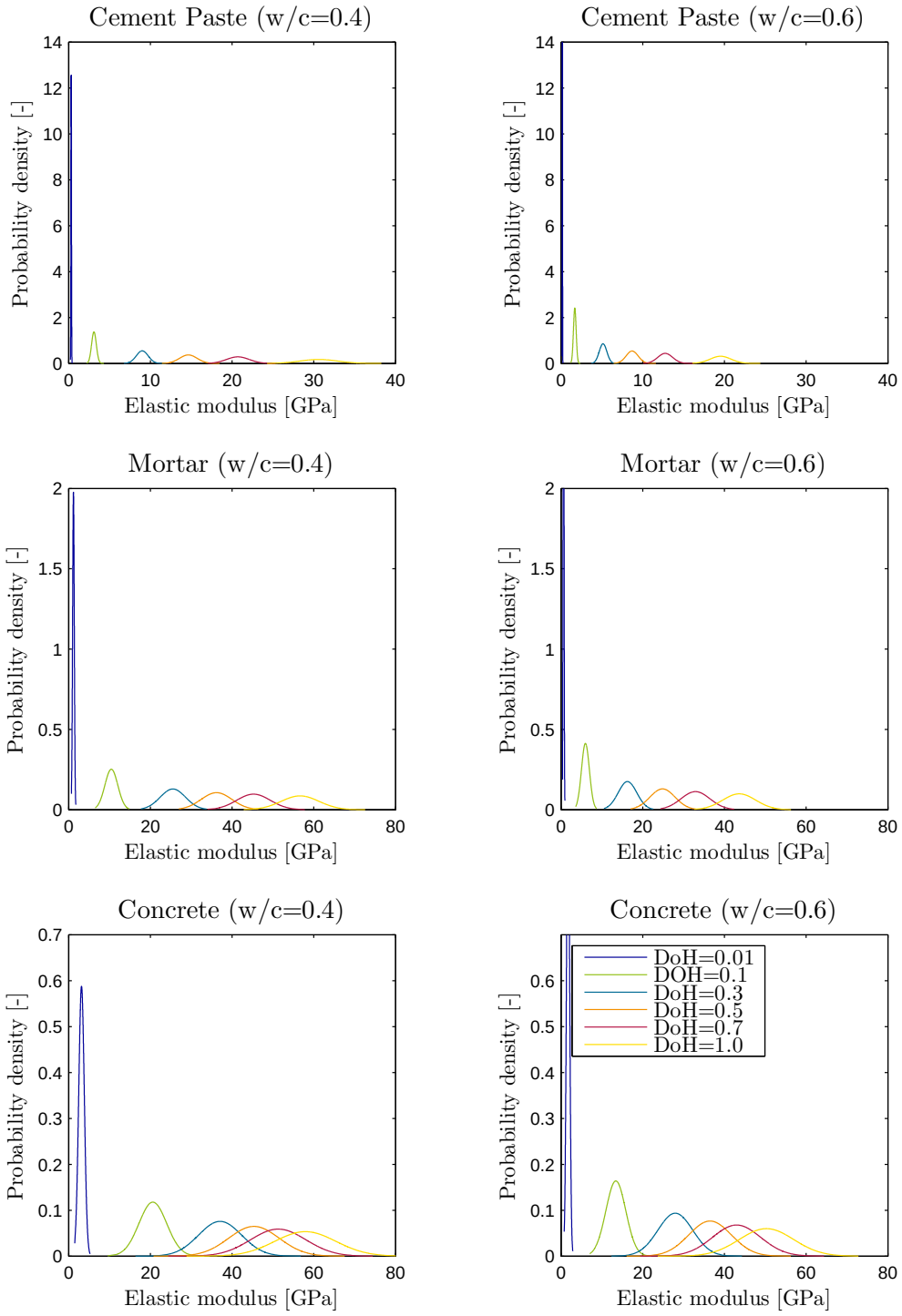

Figure 5: Probability densities of the predicted elastic modulus for the Bernard model for different degrees of hydration (DoH) as well as for different w/c-ratios at the cement paste scale, the mortar scale, and the concrete scale.

In Figure 4, the resulting probability densities of Powers' model are presented. The probability densities are shown separately for the three respective scales of observation. It is observed that the probability densities become lower during the upscaling modeling process. Furthermore, the shapes of the curves at the concrete scale are broader than at the cement paste scale. This is closely related to the evolution of the CoV as described before. Large CoV come along with broad proability density functions; both express a larger variability of the results. By showing the PDF, the differences between the results of the two different w/c-ratios are more visible than in the evolution of the CoV. The PDF shows slightly broader curves in case of a water-to-cement ratio of 0.4. One reason might be that in case of w/c=0.4 more unhydrated cement clinker particles remain in the material and thus contribute to the variation of the model results. For a water-to-cement ratio of 0.6 almost no clinker particles are left in the material. Hence, only the uncertainties of the hydration products influence the response variations.
The same conclusions can be drawn for the Bernard model. Compared to the distributions of the Powers model, the distributions of the Bernard model are slightly sharper which is related to a lower scatter in the model results. .

4.2 Sensitivity Analysis

The results of the global sensitivity analysis are exemplary discussed for the model responses using the Powers model. They are represented in Figure 6. The sum of the sensitivity indices is close to 1. Thus, interaction effects between the input parameters are negligible. The numerical effort necessary for execution of the sensitivity analysis is much higher for the Bernard model than for the Powers model due to the higher number of input parameters.

At the cement paste scale, the intrinsic elastic properties of the low-density C-S-H phase are mainly important for the model output. It is obvious that the prediction of the Young's modulus at this scale is closely related to this mechanical value since this phase represents the main component of cement paste. During the hydration process, Portlandite is formed which is linked to an increase of its sensitivity index. At the mortar scale, the volume fraction of sand is the most influencing factor whereat its influence on the model output decrease with ongoing hydration and the accompanied production of hydrates. At the concrete scale, the volume fraction of the coarse aggregates is determining at early-age hydration stages and the Young's modulus of the aggregates influences the model results in the later stages. Compared to the results for a w/c-ratio of 0.4, the results for w/c=0.6 are lower. This might be due to the fact that at the lower w/c-ratios there are some unhydrated clinker particles which also contribute to the Young‘s modulus.
The elastic properties as well as the volume fractions of the minor components do not influence the model responses much. Their sensitivity indices are mostly lower than 0.2.

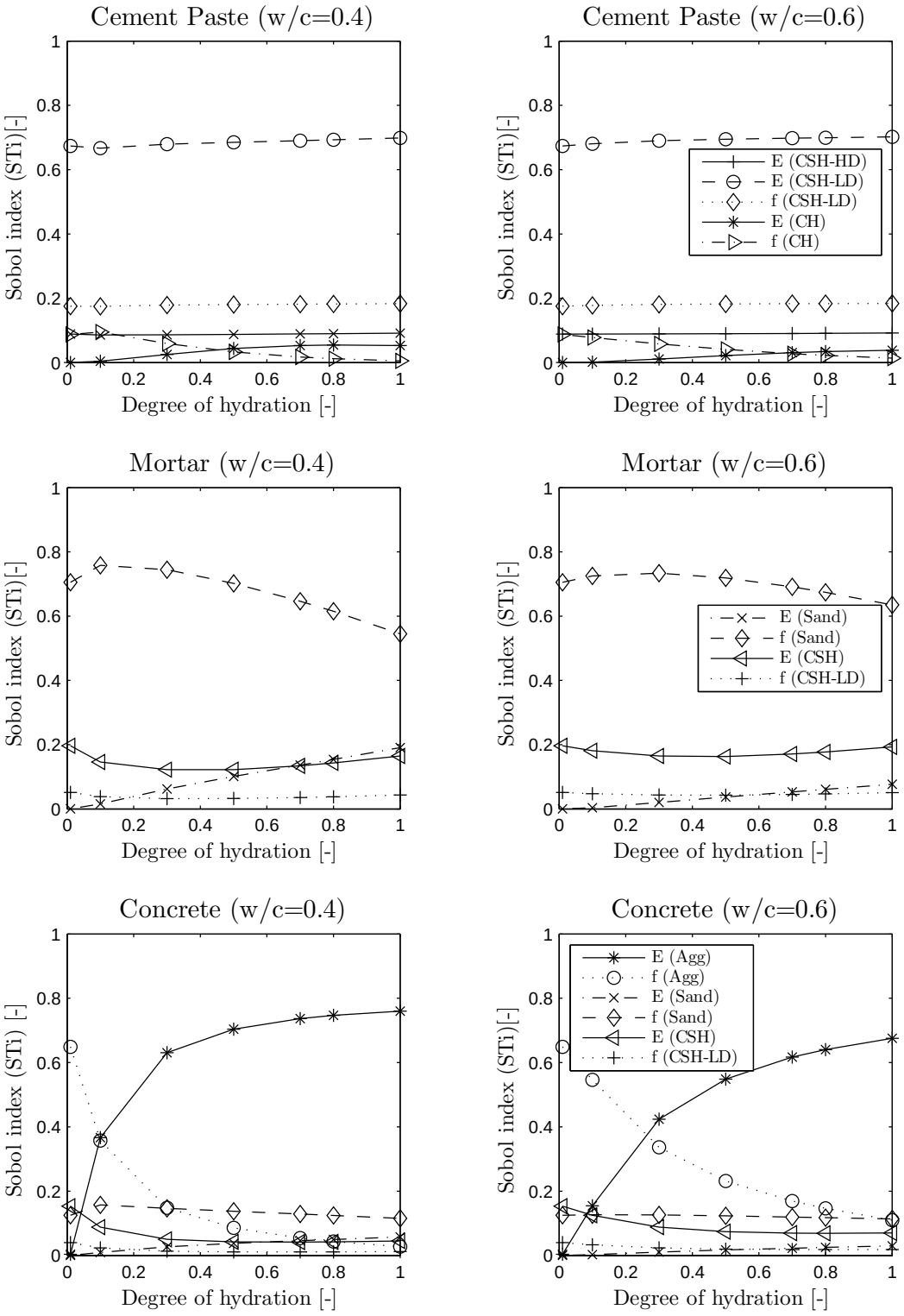

Figure 6: Evolution of total-order sensitivity indices of the Powers model as functions of the degree of hydration for two different w/c-ratios and at three scales of observation (*f – Volume fraction, E – Young's modulus, CSH-HD – C-S-H high density, CSH-LD – C-S-H low density, CH – Portlandite, Agg – Aggregate*).

5 CONCLUSION

A probabilistic approach was applied on a continuum-micromechanics based multiscale model to investigate the uncertainty propagation of input parameters across the length scales of concrete. The variability of the model responses was predicted and the parameters with the highest influence on the model outputs were identified. A probabilistic multiscale analysis through several scales of observation provides more insight on the nature of the upscaled elastic properties of cementitious materials than a deterministic analysis. Probability distributions of the model outputs and the intervals of the likelihood of the mechanical values were shown to be some of the possibilities of probabilistic model analyses.

By means of the sensitivity analysis, the significant influences of the elastic parameters at the cement paste scale and of the volume fractions at the larger scales were discussed. Furthermore, the increase of the model output uncertainties during the upscaling process as a result of the propagation of uncertainties in the input parameters was presented. In order to reduce the uncertainty of the upscaled mechanical properties of cement-based materials, the input parameters having a high sensitivity towards the Young's modulus should be determined precisely prior to the modeling process.

Comparison between the two well-known hydration kinetic models from Powers-Acker and Bernard revealed that the uncertainties and variations of both model responses are almost in the same range. The Bernard model only shows slightly higher uncertainties which seems to be surprising when the higher number of parameters in the Bernard model are considered.

This paper presented the application of a probabilistic assessment methodology on multiscale models. A further research topic could be the assessment of the accuracy of the two hydration kinetics models. It is worth to investigate whether the higher complexity of the Bernard model with its higher number of input parameter leads to an improved model prediction compared to the Powers model.

6 ACKNOWLEDGEMENTS

The research of the first author is supported by the German Research Foundation (DFG) via the Research Training Group "Evaluation of Coupled Numerical and Experimental Partial Models in Structural Engineering (GRK 1462)", which is gratefully acknowledged.

REFERENCES

[1] J. Sanahuja, L. Dormieux, and G. Chanvillard. Modelling elasticity of a hydrating cement paste. *Cement and Concrete Research*, 37(10):1427–1439, 2007.

[2] B. Pichler and C. Hellmich. Upscaling quasi-brittle strength of cement paste and mortar: A multi-scale engineering mechanics model. *Cement and Concrete Research*, 41:467–476, 2011.

[3] Chr. Pichler and R. Lackner. A multiscale creep model as basis for simulation of early-age concrete behavior. *Computers and Concrete*, 5(4):295–328, 2008.

[4] T. C. Powers and T. L. Brownyard. Studies of the physical properties of hardened portland cement paste. *Research Laboratories of the Portland Cement Association Bulletin*, 22:101–992, 1948.

[5] P. Acker. Micromechanical analysis of creep and shrinkage mechanisms. In Franz-Josef Ulm, Z. P. Bažant, and F. H. Wittmann, editors, *Creep, Shrinkage and Durability Mechanics of Concrete and Other Quasi-brittle Materials: Proceedings of the Sixth International Conference CONCREEP-6@MIT*, pages 15–26. Elsevier, 2001.

[6] O. Bernard, F.-J. Ulm, and E. Lemarchand. A multiscale micromechanics-hydration model for the early-age elastic properties of cement-based materials. *Cement and Concrete Research*, 33(9):1293–1309, 2003.

[7] Chr. Pichler, R. Lackner, and H. A. Mang. A multiscale micromechanics model for the autogenous-shrinkage deformation of early-age cement-based materials. *Engineering Fracture Mechanics*, 74(1-2):34–58, 2007.

[8] A. Clement, C. Soize, and J. Yvonnet. Uncertainty quantification in computational stochastic multiscale analysis of nonlinear elastic materials. *Computational Methods in Applied Mechanics and Engineering*, 254:61–82, 2013.

[9] N. Vu-Bac, R. Rafiee, X. Zhuang, T. Lahmer, and T. Rabczuk. Uncertainty quantification for multiscale modeling of polymer nanocomposites with correlated parameters. *Composites: Part B*, 68:446–464, 2015.

[10] M. Berveiller, Y. Le Pape, Julien Sanahuja, and A. Giorla. Sensitivity analysis and uncertainty propagation in multiscale modeling of concrete. In *Poro-Mechanics IV 2009*.

[11] N. Venkovic, L. Sorelli, B. Sudret, T. Yalamas, and R. Gagné. Uncertainty propagation of a multiscale poromechanics-hydration model for poroelastic properties of cement paste at early-age. *Probabilistic Engineering Mechanics*, 32:5–20, 2013.

[12] A. Zaoui. Continuum mechanics: A survey. *Journal of Engineering Mechanics*, 128(8):808–816, 2002.

[13] J. D. Eshelby. The determination of the elastic field of an ellipsoidal inclusion, and related problems. *The Royal Society*, 241(1226), 1957.

[14] E. Kröner. Bounds for the effective elastic moduli of disordered materials. *Journal of Mechanics and Physics of Solids*, 24:137–155, 1977.

[15] A. V. Hershey. The elasticity of an isotropic aggregate of anisotropic cubic crystals. *Journal of Applied Mechanics*, 21:236, 1954.

[16] R. Hill. Elastic properties of reinforced solids. *Journal of the Mechanics and Physics of Solids*, 11(5):357–372, 1963.

[17] G. Constantinides and F.-J. Ulm. The effect of two types of c-s-h on the elasticity of cement-based materials: Results from nanoindentation and micromechanical modeling. *Cement and Concrete Research*, 34(1):67–80, 2004.

[18] B. Pichler, S. Scheiner, and C. Hellmich. From micron-sized needle-shaped hydrates to meter-sized shotcrete tunnel shells: micromechanical upscaling of stiffness and strength of hydrating shotcrete. *Acta Geotechnica*, 3(4):273–294, 2008.

[19] V. Smilauer and Z. Bittnar. Microstructure-based micromechanical prediction of elastic properties in hydrating cement paste. *Cement and Concrete Research*, 36(9):1708–1718, 2006.

[20] W. R. Drugan and J. R. Willis. A micromechanics-based nonlocal constitutive equation and estimates of representative volume element size for elastic composites. *Journal of the Mechanics and Physics of Solids*, 44(4), 1996.

[21] P. D. Tennis and H. M. Jennings. A model for two types of calcium silicate hydrate in the microstructure of portland cement paste. *Cement and Concrete Research*, 36:855–863, 2000.

[22] T. Mori and K. Tanaka. Average stress in matrix and average elastic energy of materials with misfitting inclusions. *Acta Metallurgica*, 21(5):571–574, 1973.

[23] Y. Benveniste. A new approach to the application of mori-tanakas theory in composite materials. *Mechanics of Materials*, 6(2):147–157, 1987.

[24] A. Saltelli, M. Ratto, T. Andres, F. Campologno, J. Cariboni, D. Gatelli, M. Saisana, and S. Tarantola. *Global Sensitivity Analysis: The Primer*. John Wiley & Sons, West Sussex, England, 2008.

[25] I. M. Sobol. Sensitivity estimates for nonlinear mathematical models. *Mathematical Modelling and Computational Experiment*, 1:407–414, 1993.

[26] C. Xu and G. Z. Gertner. Uncertainty and sensitivity analysis for models with correlated parameter. *Reliability Engineering and System Safety*, 93(10):1563–1573, 2008.

[27] M. D. McKay, R. J. Beckham, and W. J. Conover. A comparison of three methods for selecting values of input variables in the analysis from a computer code. *Technometrics*, 21:239–245, 1979.

[28] P. Acker. Swelling, shrinkage and creep: a mechanical approach to cement hydration. *Materials and Structures / Concrete Science and Engineering*, 37:237–243, 2004.

[29] K. Velez, S. Maximilien, D. Damidot, G. Fantozzi, and F. Sorrentino. Determination by nanoindentation of elastic modulus and hardness of pure constituents of portland cement clinker. *Cement and Concrete Research*, 31:555–561, 2001.

[30] M. Choy, W. Cook, R. Hearmon, J. Jaffe, J. Jerphagon, and S. Kurtz. *Landolt-Bornstein: numerical data and functional relationships in science and technology. Group III: Crystal and solid state physics: Elastic, piezoelectric, pyroelectric, piezoptic, electroptic constants and nonlinear dielectric susceptibilities of crystals*, volume 11. Springer-Verlag, Berlin and Heidelberg, 1979.

A APPENDIX

A.1 Model input parameters and their stochastic properties for the Powers model

Table 1: Elastic parameters (** - assumptions).

Parameter	Mean	SD	PDF	Reference
Elastic parameters - E [GPa]				
C_3S	135	7.0	logn	ACKER [28], VELEZ [29]
C_2S	140	20.0	logn	ACKER [28], VELEZ [29]
C_3A	145	10.0	logn	ACKER [28], VELEZ [29]
C_3S	125	25.0	logn	ACKER [28], VELEZ [29]
Gypsum	45.7	4.6	logn	CHOY et al. [30]
Portlandite	38	5.0	logn	CONSTANTINIDES and ULM [17]
C-S-H-LD	21.7	2.2	logn	CONSTANTINIDES and ULM [17]
C-S-H-HD	29.4	2.4	logn	CONSTANTINIDES and ULM[17]
Sand	60	15	logn	**
Aggregate	65	20	logn	**

Table 2: Quantitative phase compositions of the reactants (** - assumptions).

Parameter	Mean	PDF	Reference
C_3S	0.622	u (0.568, 0.676)	VENKOVIC [11]
C_2S	0.152	u (0.126, 0.178)	VENKOVIC [11]
C_3A	0.106	u (0.097, 0.115)	VENKOVIC [11]
C_4AF	0.009	u (0.008, 0.010)	VENKOVIC [11]
C-S-H HD	0.7	u (0.55, 0.85)	**

Table 3: Volume fractions (** - assumptions).

Parameter	Mean	PDF	Reference
Sand content	3 u (2, 4)	**	
Aggregate content	5 u (4, 6)	**	

A.2 Model input parameters and their stochastic properties for the Bernard model

Table 4: Quantitative phase compositions of the reactants.

Parameter	Mean	PDF	Reference
C_3S	0.622	u (0.568, 0.676)	VENKOVIC [11]
C_2S	0.152	u (0.126, 0.178)	VENKOVIC [11]
C_3A	0.106	u (0.097, 0.115)	VENKOVIC [11]
C_4AF	0.009	u (0.008, 0.010)	VENKOVIC [11]

Table 5: Elastic parameters.

Parameter	Mean	SD	PDF	Reference
Elastic parameters - E [GPa]				
C_3S	135	7.0	logn	ACKER [28], VELEZ [29]
C_2S	140	20.0	logn	ACKER [28], VELEZ [29]
C_3A	145	10.0	logn	ACKER [28], VELEZ [29]
C_3S	125	25.0	logn	ACKER [28], VELEZ [29]
Gypsum	45.7	4.6	logn	CHOY et al. [30]
Portlandite	38	5.0	logn	CONSTANTINIDES and ULM [17]
C-S-H-LD	21.7	2.2	logn	CONSTANTINIDES and ULM [17]
C-S-H-HD	29.4	2.4	logn	CONSTANTINIDES and ULM[17]
Sand	60	15	logn	**
Aggregate	65	20	logn	**
Elastic parameters - ν [-] (det* - determinstic)				
C_3S	0.3		det*	ACKER [28], VELEZ [29]
C_2S	0.3		det*	ACKER [28], VELEZ [29]
C_3A	0.3		det*	ACKER [28], VELEZ [29]
C_3S	0.3		det*	ACKER [28], VELEZ [29]
Gypsum	0.33		det*	CHOY et al. [30]
Portlandite	0.305		det*	CONSTANTINIDES and ULM [17]
C-S-H-LD	0.24		det*	CONSTANTINIDES and ULM [17]
C-S-H-HD	0.24		det*	CONSTANTINIDES and ULM [17]

Table 6: Activation energies.

Parameter	Mean	PDF	Reference
Activation energies – E_{aX}/R [K]			
C_3S	4500	u (4110, 4890)	BERNARD [6]
C_2S	2500	u (2285, 2715)	BERNARD [6]
C_3A	5500	u (5025, 5975)	BERNARD [6]
C_4AF	4200	u (3835, 4565)	BERNARD [6]

Table 7: Kinetic Parameters.

Parameter	w/c-ratio	Mean	SD	PDF	Reference
Kinetic parameters: Reaction order – κ_X [-]					
C_3S	0.4	1.79	0.18	logn	BERNARD [6]
	0.5	1.72	0.17	logn	BERNARD [6]
	0.6	1.69	0.17	logn	BERNARD [6]
C_2S	0.4	1.03	0.10	logn	BERNARD [6]
	0.5	0.96	0.10	logn	BERNARD [6]
	0.6	0.90	0.10	logn	BERNARD [6]
C_3A	0.4	1.07	0.11	logn	BERNARD [6]
	0.5	1.00	0.10	logn	BERNARD [6]
	0.6	0.93	0.09	logn	BERNARD [6]
C_4AF	0.4	2.37	0.24	logn	BERNARD [6]
	0.5	2.30	0.23	logn	BERNARD [6]
	0.6	2.23	0.22	logn	BERNARD [6]
Kinetic parameters: Diffusion coefficient – D_X [-]					
C_3S	0.4	$1.05 \cdot 10^{-10}$	$0.13 \cdot 10^{-10}$	logn	BERNARD [6]
	0.5	$1.64 \cdot 10^{-10}$	$0.32 \cdot 10^{-10}$	logn	BERNARD [6]
	0.6	$6.42 \cdot 10^{-10}$	$0.77 \cdot 10^{-10}$	logn	BERNARD [6]
C_2S	0.4	$6.64 \cdot 10^{-10}$	$0.80 \cdot 10^{-10}$	logn	BERNARD [6]
	0.5	$6.64 \cdot 10^{-10}$	$0.80 \cdot 10^{-10}$	logn	BERNARD [6]
	0.6	$6.64 \cdot 10^{-10}$	$0.80 \cdot 10^{-10}$	logn	BERNARD [6]
C_3A	0.4	$2.64 \cdot 10^{-10}$	$0.32 \cdot 10^{-10}$	logn	BERNARD [6]
	0.5	$2.64 \cdot 10^{-10}$	$0.32 \cdot 10^{-10}$	logn	BERNARD [6]
	0.6	$2.64 \cdot 10^{-10}$	$0.32 \cdot 10^{-10}$	logn	BERNARD [6]
C_4AF	0.4	$1.05 \cdot 10^{-10}$	$0.13 \cdot 10^{-10}$	logn	BERNARD [6]
	0.5	$2.64 \cdot 10^{-10}$	$0.32 \cdot 10^{-10}$	logn	BERNARD [6]
	0.6	$6.42 \cdot 10^{-10}$	$0.77 \cdot 10^{-10}$	logn	BERNARD [6]

Table 8: Volume fractions (** - assumptions).

Parameter	Mean	PDF	Reference
Sand content	3	u (2, 4)	**
Aggregate content	5	u (4, 6)	**